

Article

Inducing the Effect of a Ga₂O₃ Nano-Particle on the CsF-RbF-AlF₃ Flux for Brazing Aluminum to Carbon Steels

Zhen Yao , Songbai Xue *, Jinlong Yang and Junxiong Zhang 

College of Materials Science and Technology, Nanjing University of Aeronautics and Astronautics, Nanjing 210016, China; yaozhen123@nuaa.edu.cn (Z.Y.); yangjinloong@163.com (J.Y.); zhangjunxiong126@163.com (J.Z.)

* Correspondence: xuesb@nuaa.edu.cn; Tel.: +86-025-8489-6070

Received: 15 January 2020; Accepted: 5 March 2020; Published: 7 March 2020



Abstract: In this study, a Ga₂O₃ nano-particle was added into CsF-RbF-AlF₃ flux to develop a highly active flux for brazing aluminum alloy to steel, and the spreadability and wettability of Zn-Al filler metal that matched the CsF-RbF-AlF₃ flux-doped Ga₂O₃ nano-particle on the steel were investigated. The results showed that the spreadability and wettability of the CsF-RbF-AlF₃ flux-doped Ga₂O₃ nano-particle could be remarkably improved when matching Zn-Al filler metals on both aluminum and low-carbon steel, for which the optimal content is in the range of 0.001–0.003 wt.% of Ga₂O₃. An investigation and analysis on the mechanism of reactions among CsF-RbF-AlF₃-doped Ga₂O₃ nano-particle flux and filler metal or base metals showed that the Ga₂O₃ nano-particle is selectively absorbed by the interface of molten Zn-2Al filler metal and base metal, which released the surface-active element Ga to enrich the molten Zn-2Al filler metal and decreased the interfacial tension, so as to promote the enlargement of its spreading area during the brazing process. It was concluded that adding a trace amount of Ga₂O₃ nano-particle into CsF-RbF-AlF₃ flux is a meaningful way to improve the activity of flux for brazing aluminum to steel compared with adding ZnCl₂, which poses the risk of corrosion on aluminum.

Keywords: Ga₂O₃; flux; Zn-Al filler metal; wettability; spreadability

1. Introduction

Brazing or welding Al to steel has become a hot subject in recent years because Al–steel composite metal materials have been found to have wide applications in industry. In order to develop brazing technology, the improvement of flux is a key problem that must be solved. CsF-AlF₃ eutectic flux has been widely used in brazing aluminum alloys [1] and exhibits an excellent performance in brazing dissimilar metals matched with Zn-Al filler [2,3], such as brazing Al to Al [4] and Al to Cu [5]. However, CsF-AlF₃ flux is not so good when brazing aluminum to steel, and the activity of removing the oxides on Al and steel simultaneously needs to be improved.

It was reported that matching CsF-RbF-AlF₃ flux and the 6061 aluminum alloy to 304 stainless steel can be executed [6]. According to Ref. [7], adding 6 mol.% of ZnCl₂ enhanced the activity of CsF-AlF₃ when removing the alumina during brazing. It is well known that the Cl[−] ion is a harmful ion to aluminum and steel, so developing a novel flux without a Cl[−] ion as an activator represents meaningful work.

In this paper, by adding a micro-nano Ga₂O₃ particle into an CsF-RbF-AlF₃ flux as an activator, the spreadability and wettability of Zn-Al filler metal on the aluminum, along with steel, were investigated. XDR analysis and the reaction mechanism were also studied. The results would be helpful for brazing AA5052 to Q235 steel, without the risk of Cl[−] ion corrosion.

2. Materials and Methods

The experimental base metals used for spreading tests were commercially supplied AA5052 and Q235 steel (Changshu Huayin Filler Metals Co., Ltd., Suzhou, China) with dimensions of 50 mm × 50 mm × 3 mm. The filler metal was a 2 mm diameter commercial Zn-2Al alloy wire (Zhejiang Xinrui Welding Materials Co., Ltd., Shengzhou, China). The flux used in this research was prepared using nano Ga₂O₃ powder, RbF (AR purity, Shanghai Jiuyi Chemical Reagent Company, Shanghai, China), and commercial CsF-AlF₃ flux (Zhejiang Xinrui Welding Materials Co., Ltd., Shengzhou, China). A total of 0.5 wt% of RbF and nano Ga₂O₃ powder in the range of 0.0001–0.1 wt.% were added to commercial CsF-AlF₃ flux. In order to obtain homogeneous CsF-RbF-AlF₃-xGa₂O₃ flux, accurately weighted Ga₂O₃ powder, RbF, and CsF-AlF₃ were scattered in deionized water, together with ultrasonic concussion, for an hour, in which the weight deviations of Ga₂O₃ and RbF were controlled to ±1 mg. For experimenting conveniently, all specimens were pretreated: they were degreased with acetone, oxides were removed with NaOH solution for AA5052 and HCl for Q235 steel, and the specimens were then washed with deionized water and dried naturally.

The spreading test was carried out according to China's National Standard GB/T11364-2008. A total of 0.12 g filler metal was placed on base metal, covered with the prepared CsF-RbF-AlF₃-Ga₂O₃ flux, and put into the VULCAN3-130 muffle furnace (Nanjing University of Aeronautics and Astronautics, Nanjing, China) holding at 600 °C for 60 s. To obtain accurate results, each flux was tested five times in the same conditions. The flux residue formed during the test was carefully sampled. Then, the experimental specimens were completely cleaned with hot deionized water and dried naturally. The Ga₂O₃ particle was tested by a Hitachi S-4800 SEM (Ningbo Institute of Materials Technology&Engineering, Ningbo, China), and by using the energy spectrum device (energy dispersion X-ray spectrometry, EDX) attached to the equipment, microstructure observation and joint composition analysis were carried out on the solder and joint samples. The spreading areas of filler metals were measured and calculated by Image Pro-plus software, and the flux residue was analyzed with a Bruker D8 XRD analyzer (Ningbo Institute of Materials Technology&Engineering, Ningbo, China).

3. Results and Discussion

3.1. Morphology and Size of the Ga₂O₃ Micro-Nano Particle

In order to improve the activity of CsF-RbF-AlF₃ flux, the particle size of added Ga₂O₃ has to be small enough. A range from 100 nano-meters to several microns is perfect. The size of the Ga₂O₃ particle was tested by SEM, and the results are shown in Figure 1, in which the size of the particle is below 5 μm. The EDX elemental mapping of Ga₂O₃ particles is shown in Figure 2. It was previously reported [8] that Ga₂O₃ particles presenting as short rods have more importance in the integrality of the crystal structure than those presenting as long cylinders.

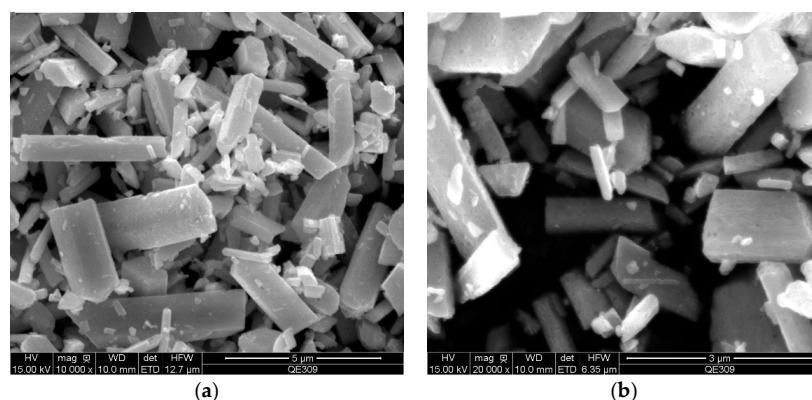


Figure 1. Morphology of Ga₂O₃ particles: (a) 10,000 times; (b) 20,000 times.

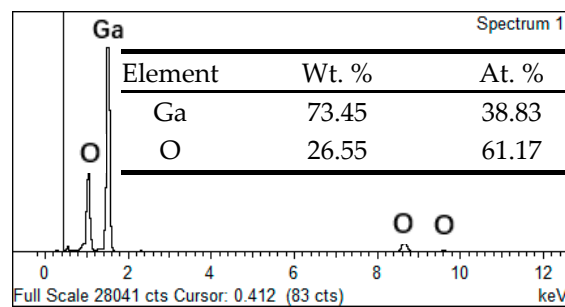


Figure 2. EDX elemental mapping of Ga_2O_3 particles.

3.2. Application Properties of the Zn-2Al Filler Metal

For determining the effect of the Ga_2O_3 particle on the spreadability and wettability of Zn-2Al filler metal, tests were carried out over 5052 aluminum and Q235 low-carbon steel with the new flux, whose spreading areas were measured and averaged. Figure 3 shows the relationship between the Ga_2O_3 concentration and spreading areas, and partial spreading tested graphs are presented in Figure 4.

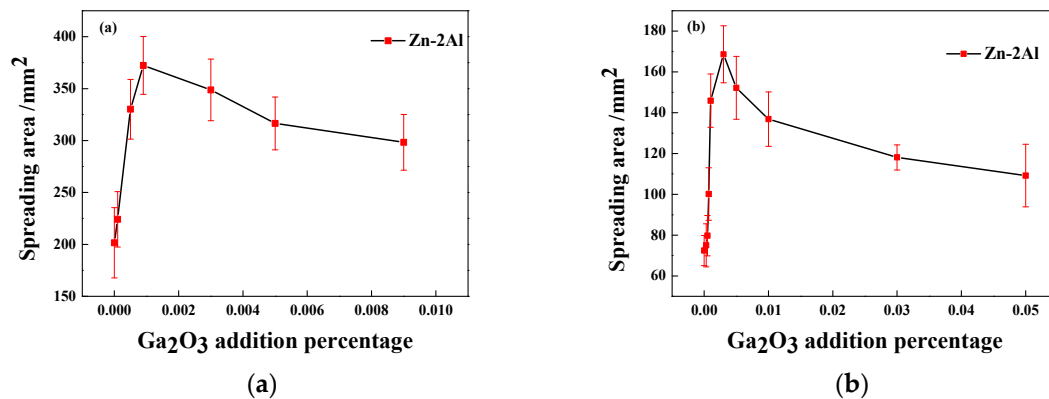


Figure 3. Effect of the Ga_2O_3 concentration on spreading areas of Zn-2Al filler metal on base metal: (a) 5052 aluminum; (b) Q235 low-carbon steel.

Figure 3 indicates that Ga_2O_3 addition to the CsF-RbF-AlF₃ flux clearly improved the spreadability and wettability of Zn-2Al filler metal on the base metal. It was found that the maximum spreading area of Zn-2Al on 5052 aluminum occurred when the concentration of Ga_2O_3 was 0.0009 wt.%. For Q235 steel, the maximum value was 0.003 wt.%. Under this circumstance, the spreading area of Zn-2Al filler metal was approximately 350 mm² over 5052 aluminum, which was an increase of 75% compared to the applications of CsF-RbF-AlF₃ flux. Additionally, it was 160 mm² over Q235 steel, representing an improvement of 122%. However, the spreading area mildly decreased with Ga_2O_3 addition continually rising. Based on the above results, the conclusion was that the CsF-RbF-AlF₃- Ga_2O_3 flux could be applied to brazing Q235 steel to AA5052 matched with Zn-2Al filler metal, and the additional concentration of Ga_2O_3 particle range was 0.0009–0.003 wt.%. In Figure 4, partial spreading images are shown. It was obvious that the spreading area of Zn-2Al filler metal was better with the Ga_2O_3 particle added in CsF-RbF-AlF₃ flux.

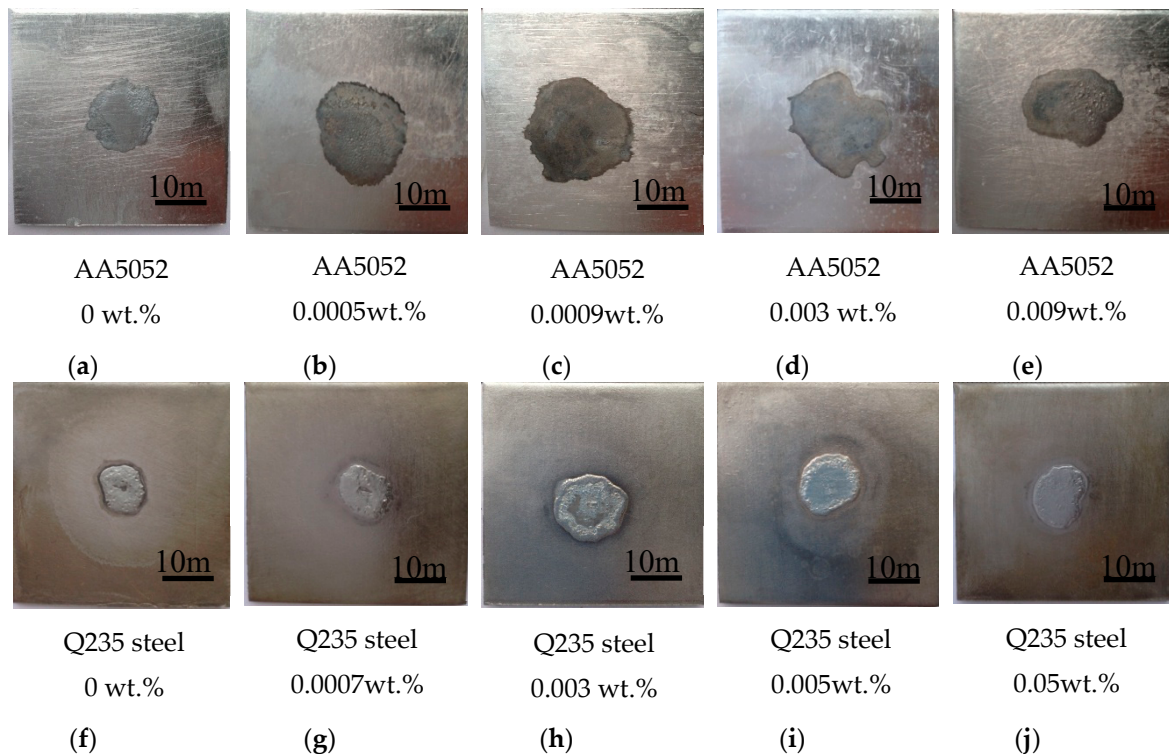


Figure 4. Spreading tests of Zn-2Al filler metal on base metals with CsF-RbF-AlF₃-xGa₂O₃ flux: (a–e) 5052 aluminum; (f–i) Q235 low-carbon steel.

3.3. Interfacial Induction Effect of the Ga₂O₃ Particle

The CsF-RbF-AlF₃-Ga₂O₃ flux improved the spreadability and wettability of Zn-2Al filler metal over 5052 aluminum and Q235 steel obviously, but the reason for this was not clear and still needed to be investigated. Therefore, we attempted to employ the theory of interfacial tension [9] to identify some explanations. According to Young's equation, the liquid balanced over a solid surface can be determined by the relationship between the interfacial tension of the solid and liquid. In this investigation, a balance of these interfacial tensions was shown between the base metal and molten flux (σ_{s-flux}), molten filler metal and molten flux (σ_{l-flux}), and base metal and molten filler metal (σ_{s-l}).

Dezellus [10] mentioned that there were two kinds of ways in which molten metal wets a solid—non-reactive wetting and reactive wetting—and the reaction of a liquid and solid decreases their interfacial tension (σ_{s-l}) to improve spreading. Because the molten flux reacted with the surface metallic oxides over the base metal to remove it, the explanation for the interfacial reactions discussed in this research was that of reactive wetting. While balancing, the relationship between interfacial tensions is in accordance with Equation (1):

$$\sigma_{s-flux} = \sigma_{l-flux} \cdot \cos \theta + \sigma_{s-l} \quad (1)$$

According to the investigation of Qian [11], alumina reacted with melted XF-AlF₃ (X = Na, K, Rb, and Cs) flux and formed AlF₃ to be dissolved, and the interfacial tension of solid–liquid (σ_{s-l}) changed from Zn-Al alloy–alumina to Zn-Al alloy–aluminum. Meanwhile, owing to the excellent intersolubility of Zn and Al [12], the interfacial tension of the AA5052 and Zn-2Al alloy (σ_{s-l}) decreased rapidly. Therefore, the spreading area of the Zn-2Al alloy over AA5052 increased obviously.

However, the surface oxide was the maximum obstacle to the brazing process for Q235 steel. No research has reported that the CsF-AlF₃ series flux reacted with iron oxidation immediately. Therefore, the reason why the Zn-Al alloy spread over Q235 should be due to the reaction between the Zn-Al alloy and oxidation. The thermodynamically calculated results shown in Table 1 indicated that iron

oxides reacted with Al to form simple substance Fe and dissolved [13]. The phase diagram of Fe-Zn showed that intermetallics, such as FeZn and FeZn₄, formed below 600 °C. Precisely because of the reaction of Zn and Fe [14], the Zn-2Al filler metal spread over Q235 steel, and their interfacial tension (σ'_{s-l}) decreased along with it.

Table 1. Reaction Gibbs energy of iron oxidation and Al (T = 873.15 K).

Compounds	Inductions	$\Delta G/\text{kJ}\cdot\text{mol}^{-1}$
FeO	Al	−259.98
Fe ₂ O ₃	Al	−811.13
Fe ₃ O ₄	Al	−1041.32
Ga ₂ O ₃	Al	−575.18

Because of the interfacial reaction, molten Zn-Al filler metal wetted the AA5052 alloy and Q235 steel and spread on them, which broke the balance of Young's equation by reducing the σ_{s-l} shown in Equations (1) and (2). When the gravity was larger than the molten flux, as shown in Table 2, the Ga₂O₃ particle settled from molten flux freely to the molten filler metal surface. According to the result of the thermodynamic calculation shown in Table 1, it was found that the Ga₂O₃ particle released Ga atoms by reacting with the Zn-Al alloy, where Ga was surface active, and could enrich the surface of filler metal to decrease its interfacial tension between metals ($\sigma'_{s-l} < \sigma_{s-l}$) [15]:

$$\sigma_{s-flux} < \sigma_{l-flux} \cdot \cos \theta + \sigma'_{s-l} \quad (2)$$

Table 2. Density of the compound.

Compound	Density/g·mL ^{−1}
Ga ₂ O ₃	6.44
CsAlF ₄	3.7

Considering the activity of molten Zn-2Al filler metal, Ga could be released and tested to demonstrate its release from Ga₂O₃. Due to having a similar property to Al [16], Ga permeated in the molten filler metal spontaneously. The microstructure at the interface of the joint is shown in Figure 5. There is no obvious defect in the interface, the filler metal is fully spread out on the surface of the Q235 steel, and the interface is well-combined. The reaction layers at the interface between the braze joint and base metal differed in thickness: the light gray layer near the braze joint and the dark gray layer near the base metal. The thickness of the interfacial IMC layer highlighted in the pictures was calculated to be 2.82 μm . The thickness of the light gray layer was 1.56 μm , and that of the dark gray layer was 1.26 μm . The EDX results in Figure 6 showed that the weak peak of Ga appeared in the interface of base metal and filler metal. With the increase of Ga₂O₃ addition, Ga₂O₃ particles displayed more activity by presenting as short rods. Owing to the decrease in σ_{s-l} , as well as the interfacial reactions, the original balance was broken and the spreading area increased obviously. A description of the variation of the interfacial tensions is shown as Figure 7. According to the Fe-Al binary phase diagram, the dark gray layer should be the θ -phase Fe-Al intermetallic compound. The θ -phase is in equilibrium with the α -Al phase in the Fe-Al phase diagram and has a monoclinic crystal structure. The atomic ratio of Al to Fe ranges from 3 to 3.5 in the θ -phase, and the crystal structure is usually represented by Fe₄Al₁₃, FeAl_{3.2}, and FeAl₃.

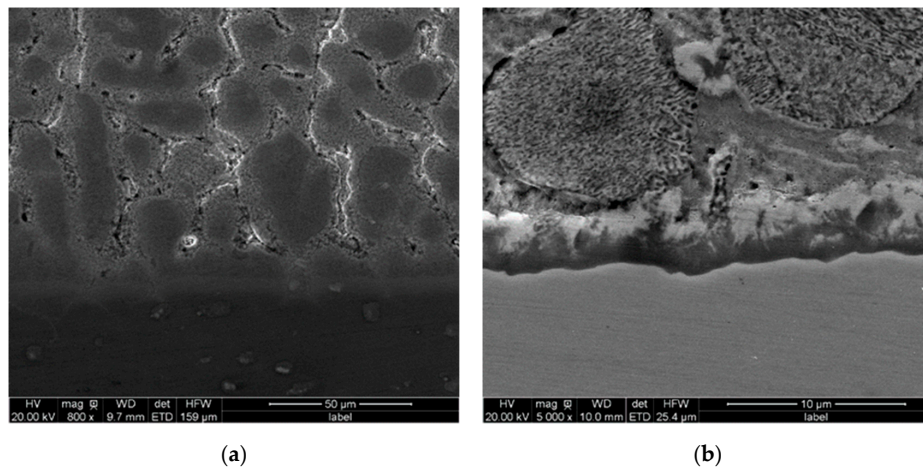


Figure 5. Microstructure at the interface of the joint: (a) 5052 aluminum; (b) Q235 low-carbon steel.

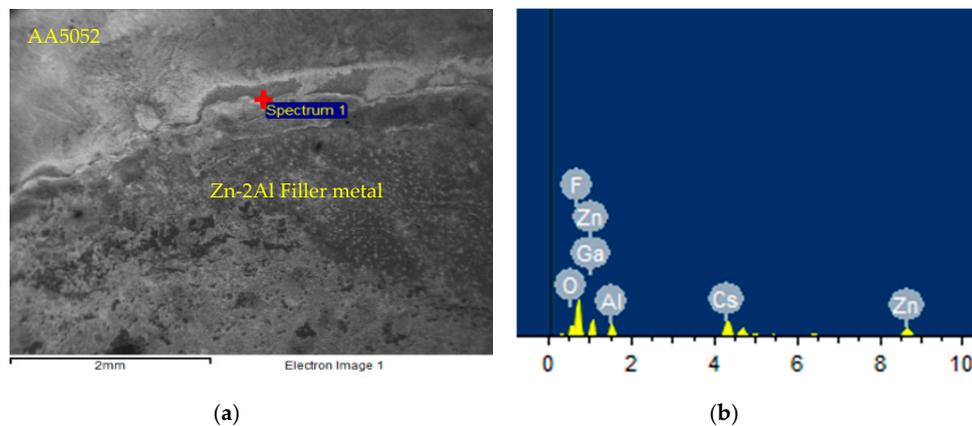


Figure 6. The interface of AA5052 and Zn-2Al filler metal: (a) SEM scanning image; (b) EDX results of the section.

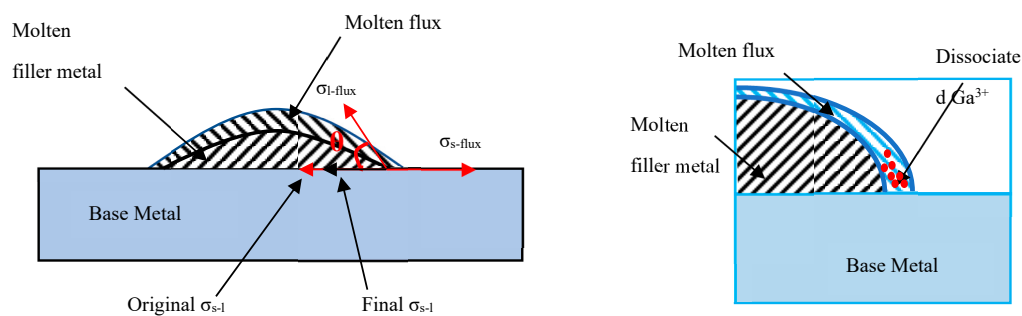


Figure 7. Diagrammatic sketch of Zn-Al spreading on base metal.

3.4. Analysis of the Flux Residue

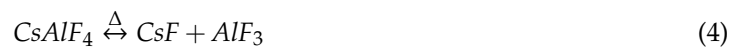
An XRD analysis experiment of the flux residue collected from the surface of AA5052 and Q235 steel was carried out. It revealed that the residue products over AA5052 were silicate, oxidation, fluoride, $\text{MgMnSi}_2\text{O}_6$, SiO_2 , Al_2SiO_5 , MgSiO_3 , Al_2O_3 , AlF_3 , MnF_2 , ZnGa_2O_4 , and Cs_{11}O_3 ; however, they were MnAlF_5 , SiO_2 , Al_2O_3 , MnF_2 , AlF_3 , ZnO , Al_2SiO_5 , AlPO_4 , and FePO_4 over Q235 steel.

According to a previous report [17], the compounds found over the AA5052 surface were mainly Mg_2Si , MgO , MgAl_2O_4 , and amorphous Al_2O_3 and a little Cu, Mn, Cr, and Fe. When heating to over 520°C , Mg, Mn, and Si were enriched. The Cs_{11}O_3 , silicate, and fluoride were from the reaction between the oxidation over the base metal and $\text{CsF-RbF-AlF}_3\text{-Ga}_2\text{O}_3$ flux. However, ZnGa_2O_4 was identified from the residue, which certainly came from the reaction of trace amounts of Ga_2O_3 in the

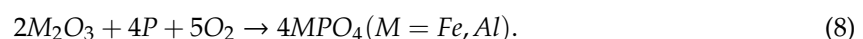
flux. It was previously reported [18] that additional Ga in the filler metal was enriched on its surface, which meant that Ga₂O₃ might have been enriched. It could be speculated that the reaction equation of ZnGa₂O₄ can be written as follows:



It was reported that the mechanism through which CsF-AlF₃ flux removed alumina was a process of dissolution and reaction, and the active ingredients were F⁻, HF, SiF₆²⁻, and Zn²⁺ ions. In this study, a massive Zn element was present in the filler metal, with a small Si element on the base metal surface, which provided the forming conditions for Zn²⁺ and SiF₆²⁻ ions during the spreading test. According to the basic principles of the chemical reaction [19], the major flux reaction was listed in Equation (4) [20]. Because of the imperfections of flux preparation technology, a trace amount of H₂O, NH₄F, and NH₄AlF₄ appeared in the CsF-RbF-AlF₃-Ga₂O₃ flux, which released active HF during the experiments and accelerated the removal of alumina:



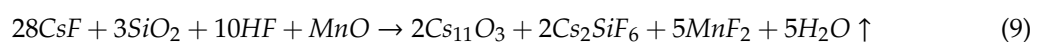
However, the XRD result of the residues over Q235 steel was not the same as that for AA5052, which included MnAlF₅, SiO₂, AlF₃, MnF₂, Al₂SiO₅, Al₂O₃, ZnO, AlPO₄, and FePO₄. Research has shown that Fe₂O₃, Fe₃O₄, and FeO orderly cover Q235 steel [21]. Therefore, iron oxide removal was the first step for brazing conveniently. It could be found that F⁻ and HF reacted with Mn compounds and AlF₃ to form MnF₂ and MnAlF₅. Fe₂SiO₅ and Al₂SiO₅ were obtained from the reaction of SiO₂ and iron oxidation and alumina. Nevertheless, a trifle phosphate, FePO₄, and AlPO₄ appeared in the XRD result. As it was shown, there was no phosphorus in the flux, whose component in Q235 was below 0.04 wt.% [22]. Therefore, FePO₄ and AlPO₄ were formed by the reactions between metallic oxides and phosphorus in Q235 steel as

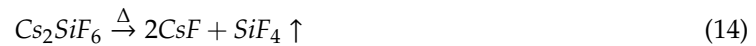
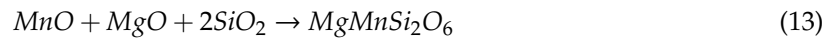
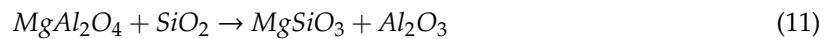


Because the content of phosphorus in Q235 was below the XRD detectability, it meant that P was enriched over the Q235 surface, which is a normal phenomenon that occurs upon heating a P-contained alloy in which phosphorus is lost through burning and phosphorus oxide is formed. Although the existence of P removed a little metallic oxide, it did not remove all oxide films. Therefore, the main reaction mechanism of removing metallic oxides was the reaction between Al and iron oxidations shown in Table 1.

It was concluded that the main reactions between the CsF-RbF-AlF₃-Ga₂O₃ flux and surface compounds on the base metal could be described as Equations (3)–(15). Due to the formation of active substances—SiF₆²⁻, HF, and F⁻—the molten flux cleaned up the surface oxidation over AA5052, and active Al in the filler metal and enriched P removed the iron oxidation over Q235 steel. Both of these mechanisms improved the spreadability and wettability of molten Zn-2Al filler metal on the base metal.

However, the reactions between silicate and metallic oxide shown in Equation (9) decreased the flux activity by consuming the CsF in CsF-AlF₃ and inhibited its flowability. Owing to the formation of Ga, the spreadability and wettability of Zn-2Al filler metal were enhanced, despite the activity loss:





According to the proposed mechanisms, it was indicated that molten flux reacted with oxidation over base metals to promote the spread of filler metal simultaneously. However, the rapidly effectiveness loss of molten flux decreased the efficiency of alumina removal and further strangled the spreading speed of filler metal, which was mainly due to the consumption of active substances— SiF_6^{2-} , HF, and F^- —and the appearance of silicates.

Compared to the lower efficiency of CsF-RbF-AlF₃ flux on iron oxidation, the Ga₂O₃ addition obviously improved the activity of the flux because of its enrichment and production of Ga, which helped to decrease the interfacial tension between base metal and molten filler metal. Meanwhile, Ga₂O₃ partially reacted with ZnO to dissolve it, in order to promote the further spreading of molten Zn-2Al filler on the base metal.

4. Conclusions

In this study, it was demonstrated that the activity of CsF-RbF-AlF₃ flux was clearly enhanced by adding a trace amount of Ga₂O₃, promoting the further enlargement of the spreading area of the Zn-2Al filler metal over AA5052 and Q235 steel. The major conclusions were as follows.

The spreading tests showed that the addition of trace amounts of Ga₂O₃ in CsF-RbF-AlF₃ flux promoted the enlargement of the spreading area of Zn-2Al filler metal on both Q235 steel and AA5052 matrix, and the optimal content of Ga₂O₃ was 0.001–0.003 wt.%.

The interfacial effect and induction effect of Ga₂O₃ improved the flux activity by reacting with Al atoms to provide Ga and enriched molten filler metal to decrease its interfacial tension and promote the spreading area increase of molten Zn-2Al filler metal over the matrix. Meanwhile, the phosphorus oxidation and active Al removed iron oxidation and effectively increased the spreading area of molten Zn-2Al filler metal over the Q235 steel matrix.

As a result of the identified reaction mechanism, it was found that Ga₂O₃ partially reacted with ZnO and slowed down the efficiency loss speed of CsF-RbF-AlF₃ flux to improve its flowability.

Author Contributions: Conceptualization, S.X.; methodology, J.Z.; software, Z.Y.; validation, Z.Y.; formal analysis, Z.Y.; investigation, Z.Y.; resources, S.X.; data curation, Z.Y.; writing—original draft preparation, Z.Y.; writing—review and editing, Z.Y.; visualization, Z.Y.; supervision, J.Y.; project administration, J.Y.; funding acquisition, S.X. All authors have read and agreed to the published version of the manuscript.

Funding: This work was funded by the National Natural Science Foundation of China, Grant No. 51375233 and the Priority Academic Program Development of Jiangsu Higher Education Institutions (PAPD).

Acknowledgments: We gratefully acknowledge the support of Jiangsu Higher Education Institutions for providing a scholarship for Zhen Yao. Songbai Xue acknowledges financial support from the National Natural Science Foundation of China, Grant No. 51375233.

Conflicts of Interest: The authors declare no conflicts of interest.

References

1. Cheng, F.J.; Yang, J.X.; Zhao, H.W.; Zhang, G.X.; Huang, J.L.; Long, W.M. Relationship between phase structure and melting characteristics of low cesium KF-CsF-AlF₃ aluminum flux. *Trans. China Weld. Inst.* **2013**, *34*, 5–8.

2. Cheng, F.J.; Jin, W.S.; Wang, Y.; Wang, D.P. The Chemical Reactions in Solution Synthesis of Aluminum Alloy Brazing Fluoride Flux. *Adv. Mater. Res.* **2011**, *291*, 924–928. [[CrossRef](#)]
3. Xu, Z.W.; Yan, J.C.; Wang, C.; Yang, S.Q. Substrate oxide undermining by a Zn–Al alloy during wetting of alumina reinforced 6061 Al matrix composite. *Mater. Chem. Phys.* **2008**, *112*, 831–837. [[CrossRef](#)]
4. Luo, W.; Wang, L.T.; Wang, Q.M.; Gong, H.L.; Yan, M. A new filler metal with low contents of Cu for high strength aluminum alloy brazed joints. *Mater. Des.* **2014**, *63*, 263–269. [[CrossRef](#)]
5. Ji, F.; Xue, S.B.; Dai, W. Reliability studies of Cu/Al joints brazed with Zn–Al–Ce filler metals. *Mater. Des.* **2012**, *42*, 156–163.
6. Yang, J.L.; Xue, S.B.; Xue, P.; Lv, Z.P.; Dai, W.; Zhang, J.X. Development of novel CsF–RbF–AlF₃ flux for brazing aluminum to stainless steel with Zn–Al filler metal. *Mater. Des.* **2014**, *64*, 110–115. [[CrossRef](#)]
7. Xiao, B.; Wang, D.P.; Cheng, F.J.; Wang, Y. Oxide film on 5052 aluminium alloy: Its structure and removal mechanism by activated CsF–AlF₃ flux in brazing. *Appl. Surf. Sci.* **2015**, *337*, 208–215. [[CrossRef](#)]
8. Ma, F.; He, J.H.; Liang, C. Influence of Ga₂O₃ Morphology on Synthesis of YAGG: Ce³⁺ Phosphor Powders by Solid-state Reaction Method. *Guangzhou Chem. Ind. Technol.* **2018**, *19*, 36–38.
9. Weber, C.; Stanjek, H. Energetic and entropic contributions to the work of adhesion in two-component, three-phase solid–liquid–vapour systems. *Coll. Surf. A Physicochem. Eng. Asp.* **2014**, *441*, 331–339. [[CrossRef](#)]
10. Dezellus, O.; Eustathopoulos, N. Fundamental issues of reactive wetting by liquid metals. *J. Mater. Sci.* **2010**, *45*, 4256–4264. [[CrossRef](#)]
11. Qian, H.; GAO, H.; Sun, B. Recent Researches and Development of Brazing Flux for Aluminum. *Mater. Rev.* **2007**, *12*, 76–78.
12. Osório, W.R.; Garcia, A. Modeling dendritic structure and mechanical properties of Zn–Al alloys as a function of solidification conditions. *Mater. Sci. Eng. A* **2002**, *325*, 103–111. [[CrossRef](#)]
13. Fan, R.H.; Lv, H.L.; Sun, K.N.; Wang, W.X.; Yi, X.B. Kinetics of thermite reaction in Al–Fe₂O₃ system. *Thermochim. Acta* **2006**, *440*, 129–131. [[CrossRef](#)]
14. Dong, H.; Yang, L.; Dong, C.; Kou, S. Improving arc joining of Al to steel and Al to stainless steel. *Mater. Sci. Eng. A* **2012**, *534*, 424–435. [[CrossRef](#)]
15. Zhao, H.T.; Shi, Y.Q.; Tian, M. Investigation on the Effect of the Substrate Temperature on the Photoelectric Properties of the Ga Doped ZnO Film. *Mater. Sci. Forum* **2016**, *852*, 1066–1069. [[CrossRef](#)]
16. Guo, S.L.; Li, D.F.; Wu, X.P.; Xu, X.Q.; Du, P.; Hu, J. Characterization of hot deformation behavior of a Zn–10.2Al–2.1Cu alloy using processing maps. *Mater. Des.* **2012**, *41*, 158–166. [[CrossRef](#)]
17. Zhang, J.X.; Xue, S.B.; Xue, P.; Liu, S. Thermodynamic reaction mechanism of the intermetallic compounds of Sn_xNd_y and Ga_xNd_y in soldered joint of Sn–9Zn–1Ga–0.5Nd. *J. Mater. Sci. Mater. Electron.* **2015**, *26*, 3064–3068. [[CrossRef](#)]
18. Zhu, H.; Xue, S.B.; Sheng, Z. Effect of alloying elements on intermediate temperature filler metal in stepped welding of 6063 aluminum alloy. *Trans. China Weld. Inst.* **2009**, *30*, 33–36.
19. Khan, T.I.; Kabir, M.H.; Bulpett, R. Effect of transient liquid-phase bonding variables on the properties of a micro-duplex stainless steel. *Mater. Sci. Eng. A* **2004**, *372*, 290–295. [[CrossRef](#)]
20. Davies, G.B.; Krüger, T.; Coveney, P.V.; Harting, J.; Bresme, F. Interface deformations affect the orientation transition of magnetic ellipsoidal particles adsorbed at fluid–fluid interfaces. *Soft Matter* **2014**, *10*, 6742–6748. [[CrossRef](#)]
21. Wan, Y.; Zhang, D.; Liu, H.Q.; Li, Y.J.; Hou, B.R. Influence of sulphate-reducing bacteria on environmental parameters and marine corrosion behavior of Q235 steel in aerobic conditions. *Electrochim. Acta.* **2010**, *55*, 1528–1534. [[CrossRef](#)]
22. Wang, X.; Yan, Q.; Li, X. Microstructure and properties of 20 steel pipe joints by transient liquid phase bonding and high temperature brazing. *Trans. China Weld. Inst.* **2005**, *26*, 56–60.

